COMITATO NAZIONALE PER L'ENERGIA NUCLEARE
Laboratori Nazionali di Frascati

LNF - 64/46
15 Settembre 1964.

R. Habel, T. Letardi and R. Visentin: CONSTRUCTION AND OPERATION OF A SINGLE GAP SPARK CHAMBER. -

Servizio Documentazione
dei Laboratori Nazionali di Frascati del CNEN
Casella Postale 70 - Frascati (Roma)

Laboratori Nazionali di Frascati del CNEN
Servizio Documentazione

LNF - 64/46

Nota interna: n. 258
15 Settembre 1964.

R. Habel, T. Letardi and R. Visentin: CONSTRUCTION AND OPERATION OF A SINGLE GAP SPARK CHAMBER. -

Introduction. -

Recent works[1] on spark chambers showed the possibility of employing single-gap spark chambers (10 - 30 cm wide plate to plate) to detect charged particles.

The amount of information available from photographs of tracks in this chamber is, under many respects, equivalent and even better than the information available from the tracks photographed in the common narrow-gap spark chambers with similar dimensions.

The absorbing layer in the single-gap chamber may be minimized and tracks forming angles from 0^o to 40^o with the pulsed electric field E can be detected, without apparent loss of efficiency of detection.

The practical realisation of this kind of detector is very easy, because of the smaller accuracy needed in mounting conducting plates at the correct distance and in preparing their surfaces, so as to obtain a good detection efficiency. Efficiency depends on gas purity. Edge sparks are avoided by care in cleaning the internal walls and rounding all protruding edges.

Single-gap spark chamber construction. -

We built the chamber with the following dimensions; distance between conducting plates (Al, 2 cm thick) d = 22 cm, cross section 20×20 cm^2.

The transparent lucite walls are 2.5 cm thick. The metallic plates are screwed to the lucite walls, and vacuum tightness is assured by rubber gaskets. The thickness of the walls allows us to make observations in a wide range of pressures.

Experimental arrangement. -

The coincidence pulse between two scintillation counters defines a charged particle (cosmic ray) crossing the chamber.

Simultaneously a spark-gap pulse fires a pulse voltage multiplier of the Marx type (fig. 1a), with 25 K. V. d. c. supply, capable of delivering a maximum nominal pulse amplitude of 200 KV.

In the scheme of fig. 1b, the C_M condenser, circuital equivalent of the voltage multiplier, is initially charged to the high voltage V_o (60 - 200 KV); when I closes the high voltage circuit a pulse V is applied to the chamber (condenser C_c) through the series resistor R_s. C_c is shunted by resistor R_d.

The total delay, between the crossing of the particle through scintillation counters and the high voltage pulse is actually 300 ns, and can be minimized when the H. V. Multiplier spark gaps are properly adjusted near breakdown.

The rise time of the V_o pulse is a few nanoseconds, if $R_s = 0$(x).

The shunting resistor R_d brings to zero the amplitude of the V_o pulse in a sufficiently short time (200 - 300 ns).

Employed gases. -

The following photographs are related to observations made with pure neon in the chamber. We also employed a Ar (5 %), Ne (95 %) mixture, but the observations are not reported because still incomplete.

Observations in Ne or He. -

In the normal arrangement of the chamber the tracks make an angle $\leq 40^o$ with the direction of the electric field E.

Such a situation is shown in fig. 2.

The negative pulse V_o is applied to the upper plate. The discharge initially follows for about 1 cm the electric field lines (this effect is marked near the upper plate) then joins the primary ionized path.

Such a behaviour is in agreement with the observations of other workers[2] and with the description of the discharge mechanism[3]. We want to remark that the track is formed also if it does'nt cross both the conducting plates, penetrating through one of the side (lucite) walls.

Assuming as independent parameters either R_d, R_s, p (gas pressure) or V_o, we made observations to correlate the detection efficiency, the brightness and the track thickness with the change of the above quantities. When R_d is larger than 1 Kohm andthe other parameters a-

---

(x) - We neglect in all cases the sparks resistence in the H. V. multiplier.

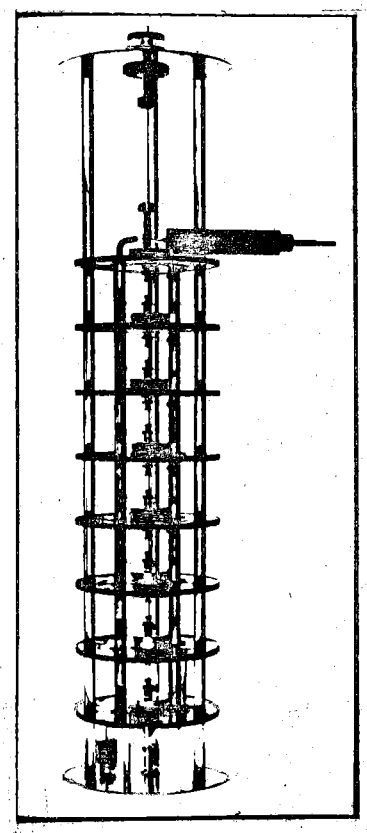

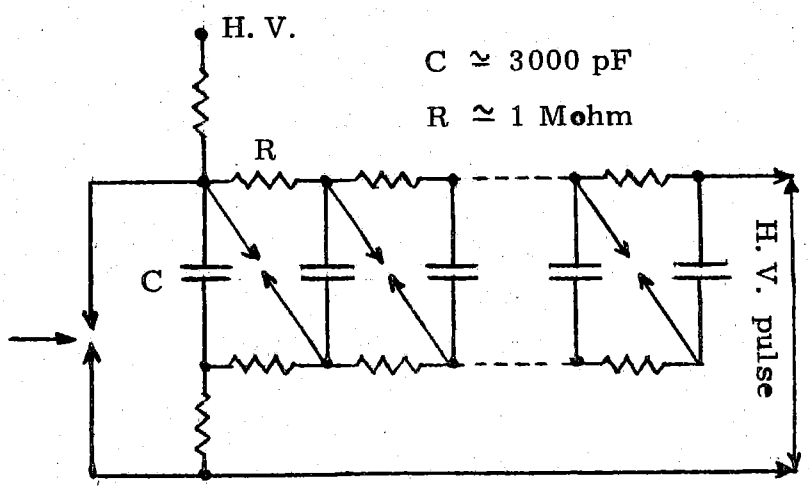

FIG. 1 a

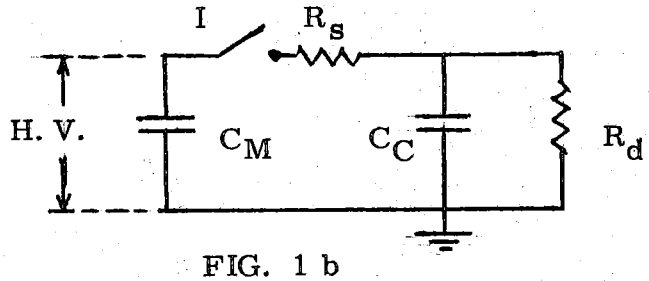

FIG. 1 b

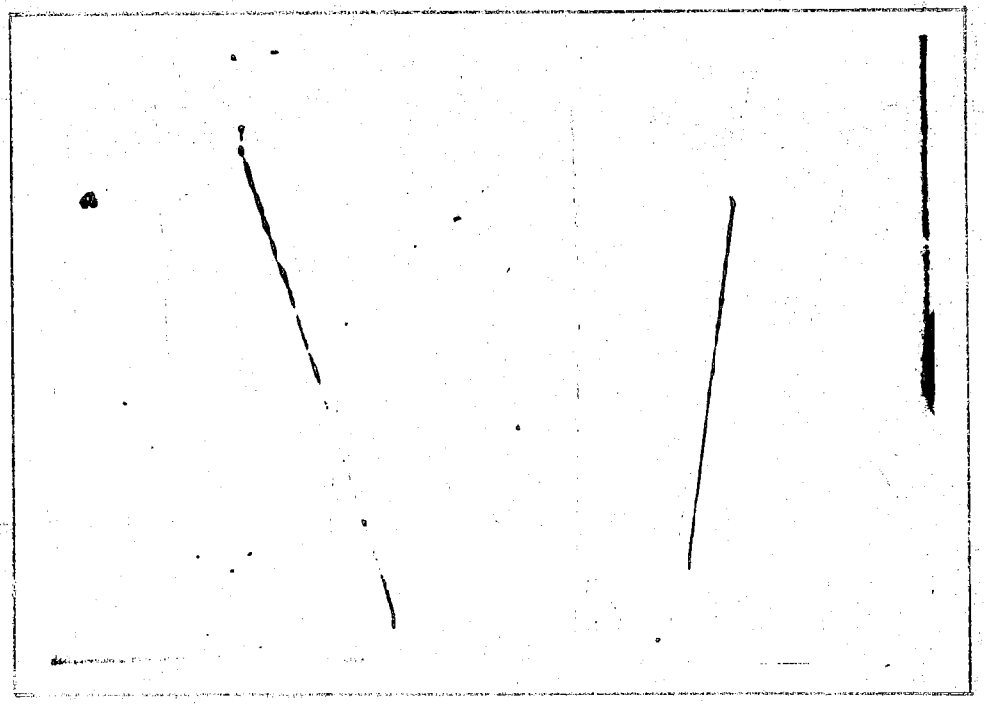

Gas Ne p ≅ 1 atm
TRIX F/11 D = 1.5 m

FIG. 2

re kept fixed at ordinary values (see below), the brightness and detection efficiency of the tracks are not affected by the value of R_d. When R_d is decreased below 1 Kohm the above characteristics rapidly decrease and are practically zero when $R_d = 0.5$ Kohm.

The time constant of the decaying part of the pulse V_o applied to the chamber is

$$\tau_d = R_d (C_M + C_c) \simeq R_d C_M$$

where C_M is the total capacitance of the multiplier. When $R_s = 0$, $R_d = 0.5$ Kohm, $C_M \sim 400$ pF we have $\tau_d \sim 400$ ns.

When $R_d \sim 1$ Kohm the amplitude of the pulse V_o, for which the efficiency is zero in Ne, is $V_o \sim 50$ KV (E = 2.5 KV/cm).

When the pulse V_o is 100 KV, the pulse lenght must be $\gtrsim 200$ ns for non zero efficiency.

The series resistor R_s limits the current during the discharge, thus acting on the spark thickness.

Fig. 3 qualitatively shows the dependence of the track thickness (s in mm) from R_s.

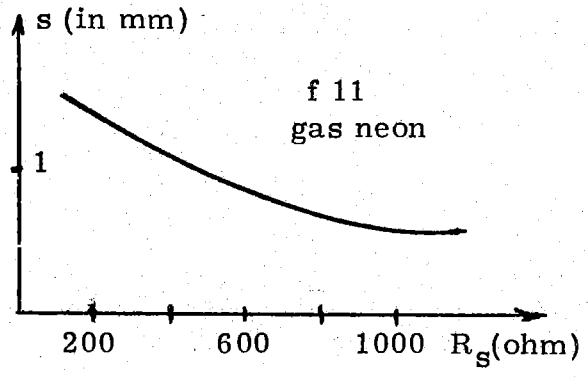

FIG. 3

With values of R_s above 1 Kohm, the track brightness is so low that the camera lens must be used at very large f-number (f/2.8 with Kodak trix film) causing an important decrease of the field depth. The detection efficiency is however independent of R_s, in a large range of values.

We made observations to establish the dependence of the detection efficiency on V_o and p.

The curves of figg. 4 and 5 show the results of the observations in two particular cases.

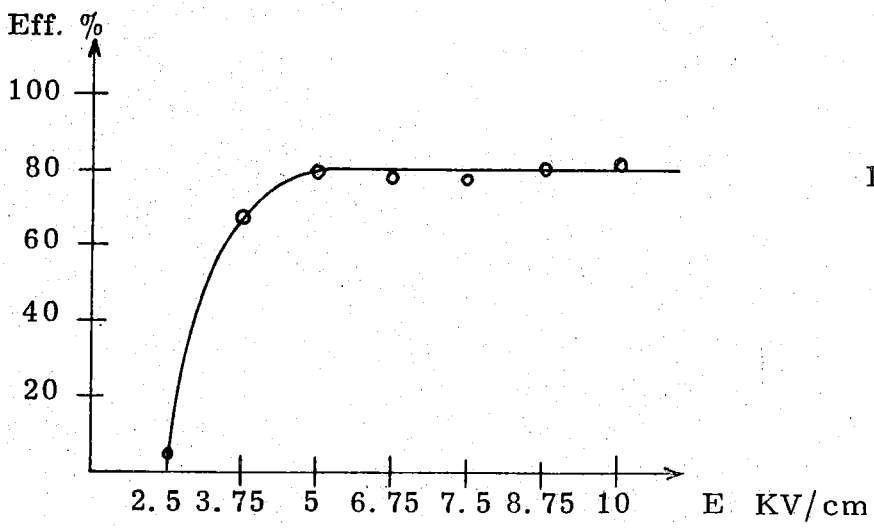

FIG. 4

We define the detection efficiency through the ratio between the number of events in which we can unambiguously recognize a particle track (fig. 2) which has crossed both the scintillation counters, and the total number of coincidence events.

From fig. 4 we see that the efficiency is constant at a value around 78 % for a wide range of values of the electric field and of the pressure. With a better experimental apparatus connected to the same chamber (for instance a threefold coincidence, required for defining a particle in the chamber) we think that measured efficiency should be even better. Of course in the practical use of sparks chambers the working parameters will be fixed in such a way to have optimum conditions for both efficiency and resolution of tracks pictures.

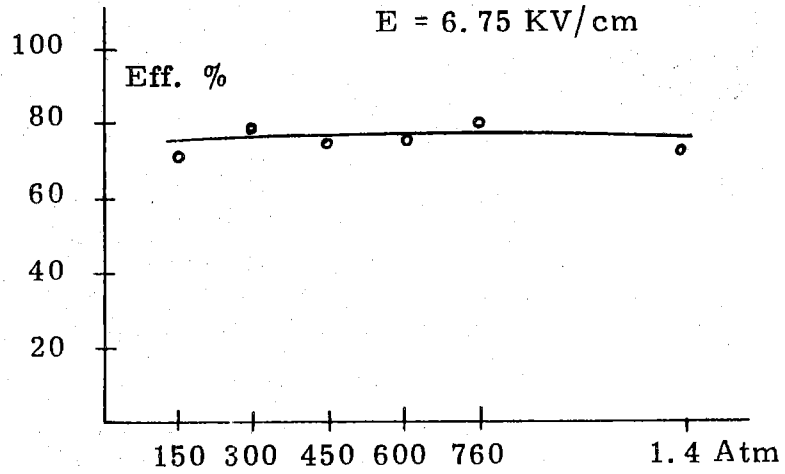

FIG. 5

Figg. 6 and 7 allows us to correlate the track thickness with the amplitude of V_o pulses and pressure p.

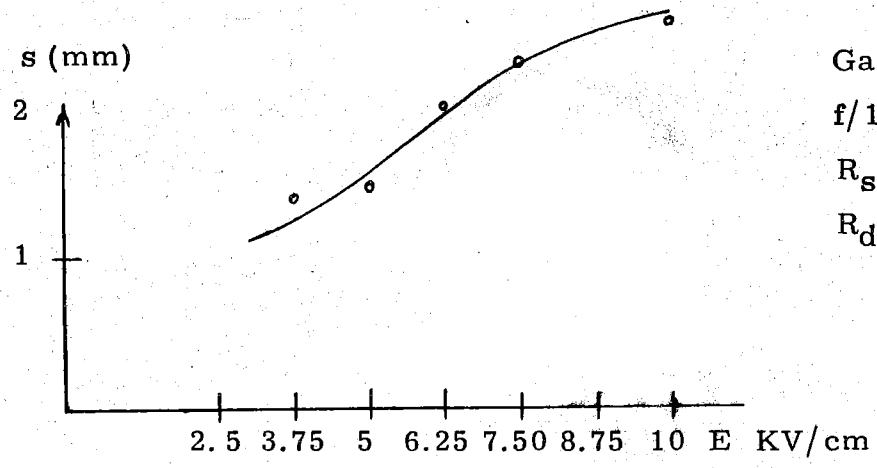

Gas He
f/16 p = 1.1 atm
R_s = 300 ohm
$R_d \simeq$ 5 Kohm

FIG. 6

The conditions of normal operation are taken as being given by the following values of the parameters: p = 1 atm, R_s = 300 ohm, R_d = 5 Kohm; we then may determine V_o from figg. 6 and 4.

We have made observations to express the efficiency as function of the delay Δt between the coincidence and the V_o pulses, without clearing field. The efficiency showed no appreciable variation with delays Δt of about 1.5 - 2 μs. Even with delays of about 4 μs it however remained appreciably different from zero.

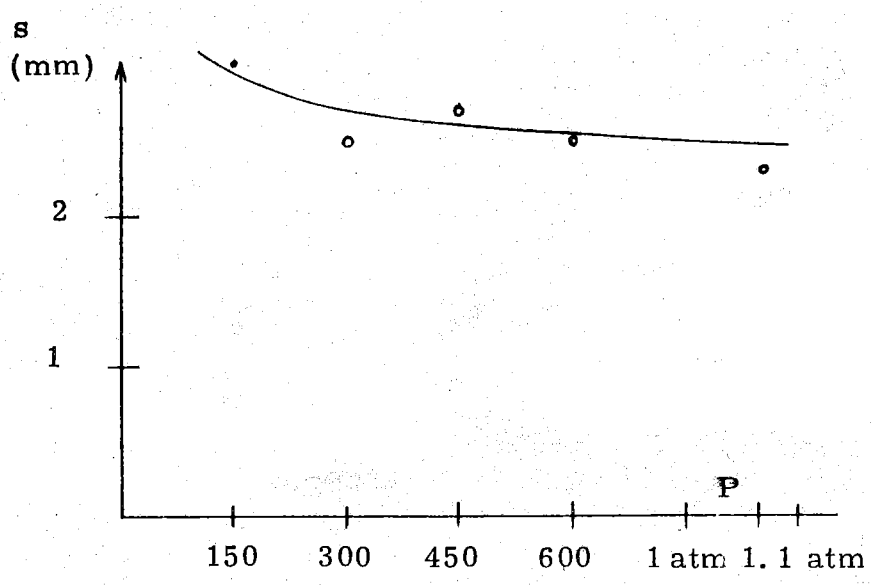

Gas He
f/16
E = 7.50 KV/cm
R_s = 300 ohm
R_d - 5 Kohm

FIG. 7

Tracks forming an angle $\geq 40^{o}$ with E. -

It is well known that when a charged particle crosses the volume of a spark chamber, forming an angle $\varphi \geq 40^{o}$ with E, the usual spark breaks into streamers[4], following field direction from one conducting plate to the other, these streamers laying in a plane containing the particle path.

If one of the conducting plates is transparent, the projection of the particle path on a plane orthogonal to the electric field may be photographed.

To verify the above results reported by the quoted authors, and not being in posses of a transparent conducting plate, we have arranged the photographic apparatus as shown in fig. 8. (Particles normally incident to the figure plane).

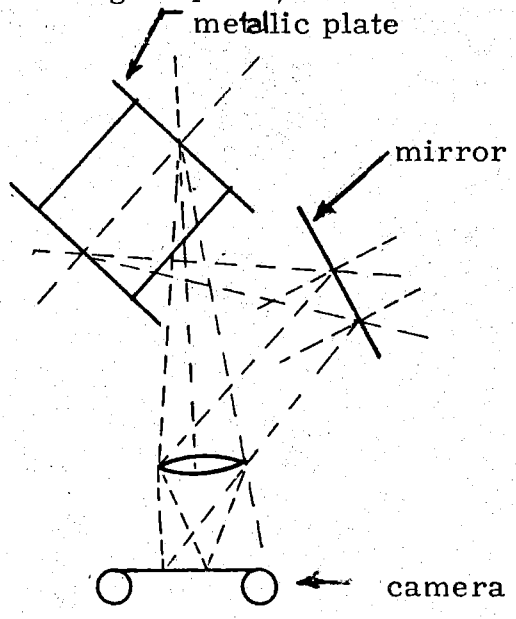

FIG. 8

As can be deduced from fig. 9, where (see fig. 8) the left side is the positive plate of the spark chamber, reflected in the mirror, the right one is the direct sight of the negative one, the streamers end in a disordered way on the negative pulsed plate, while on the grounded (positive) plate the end points of the streamers are well allined along the orthogonal projection of the particle path on the plate.

In the same picture we can see, in a plane with the streamers, a straight line of brightspots, which, as can be seen observing the successive picture (see further explanation below), a

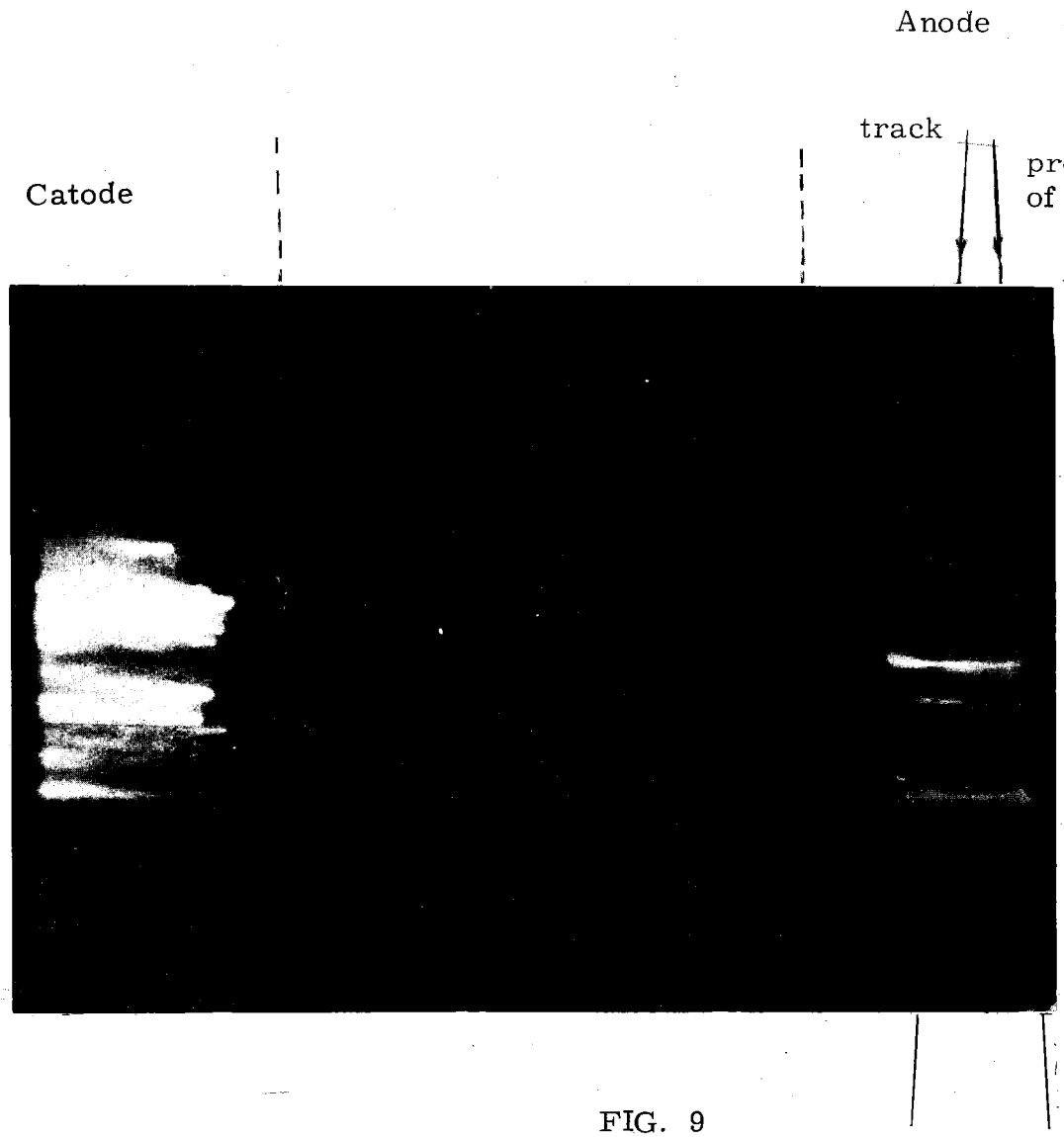

FIG. 9

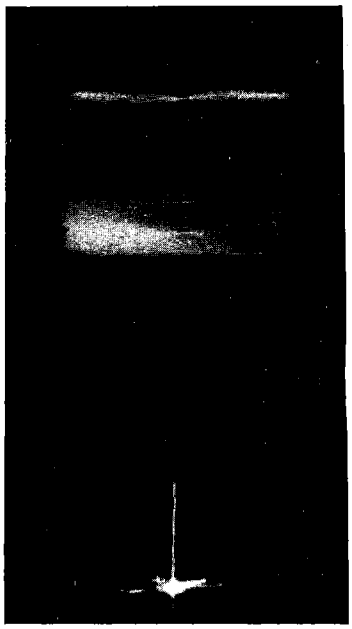

Gas He p ≃ 1 atm

TRIX F/8 D = 1.5 m

FIG. 10

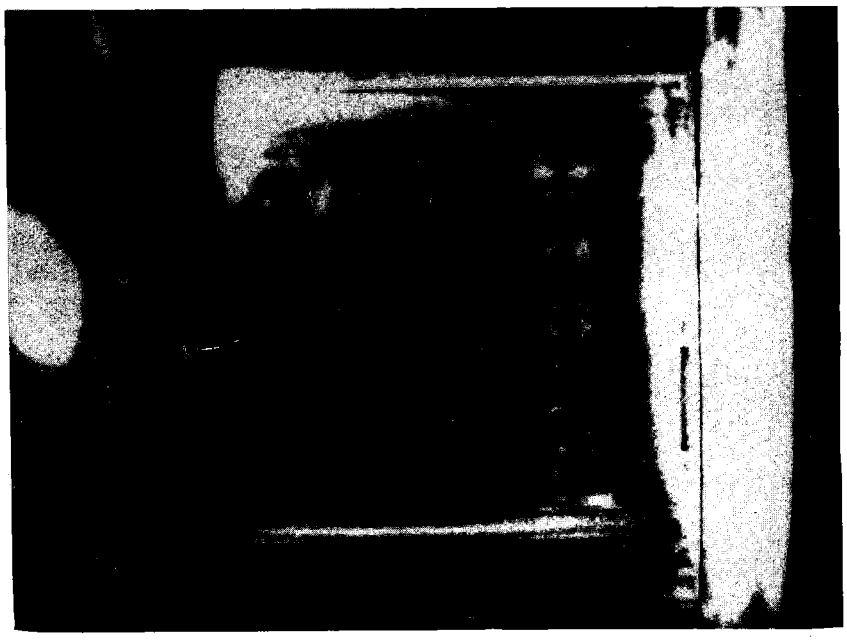

a)

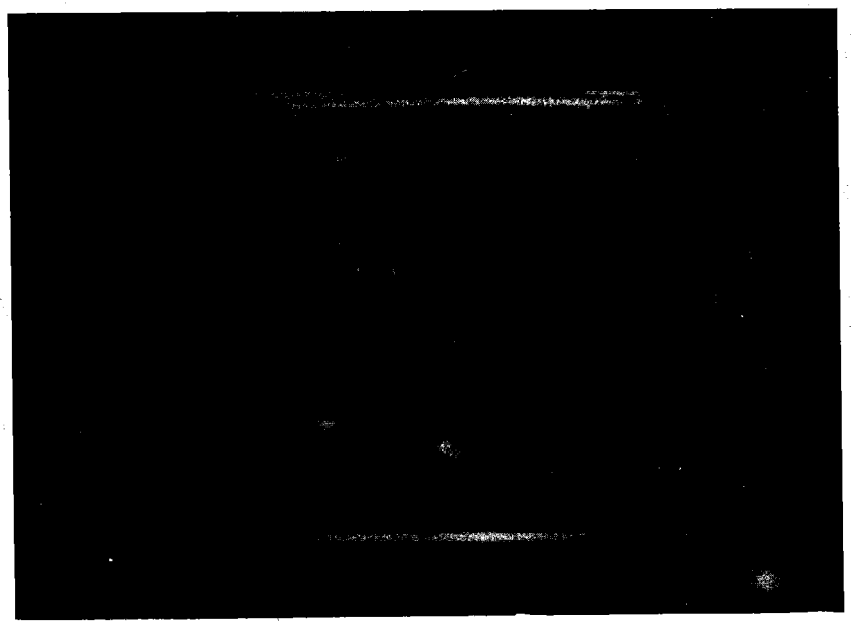

b)

FIG. 11

re in line with the primary ionization track produced by the particle.

In this way from both the front and projected picture we have complete information about the spatial coordinates of the particle path, though not so accurate as in the ordinary case ($\theta \lesssim 40^{o}$).

To show that the straight line individuated by the bright spots is the path of the particle, we have placed two chambers, one above the other, the upper to detect the particle in the ordinary conditions ($\theta \lesssim 40^{o}$), the lower placed with the conducting plates parallel to the selected directions of the particles (see fig. 10). The upper part of the picture shows the track of the impinging particle obtained in the ordinary way, while the lower one shows it defined by the bright spots across the streamers plane. The V_0 pulse is fed to the two chambers in parallel.

The voltage and the pressure conditions for a good efficiency, when the chamber is operated with the electric field normal to the particle path (in this arrangement), are dependent on the employed gas. Filling the chamber with Ne and varying the pressure in the range of 150 mmHg - - 1.5 atm, with the pulse amplitude kept constant at 125 KV, we don't observe substantial variations in the operating mode. If the employed gas is He, the pressure must be kept less than 1 atm (150 - 600 mmHg), when the pulse amplitude is $\sim$ 200 KV.

Rising the pressure, pulses larger than 200 KV are needed.

We have made some measurements to establish a possible correlation between the primary ionization the loss of energy of the particle, and the number of bright spots.

Shielding completely one of the scintillation counters with a 10 cm thick Pb slab, we selected high energy cosmic rays which had crossed the chamber. In figg. 12 a and b are plotted the distributions of the number of bright spots we have obtained in two different conditions (gas Ne; p = = 1.1 atm (fig. 12a), and p = 1.6 atm (fig. 12b)).

The reading difficulty of the photograms increases with the mean number of bright spots, because the pictures could not be made with the same resolution as in ordinary tracks, the brightness of the tracks being much smaller.

The resolution for the spatial definition of the tracks in fig. 10 is better if the V_0 pulse has rectangular shape and is short ($\sim$40 ns)[5].

When the chamber is pulsed with the scheme of fig. 1, the amplitude of V_0 decays exponentially. To realize the rectangular pulse we have placed in parallel with the chamber a spark gap, which short circuits the plates about 30 - 50 ns after the high voltage pulse has been applied.

Shaping the pulse and filling the chamber with Ne (1.1 atm) it has been possible to observe particle tracks orthogonal to the field, without the streamers, normally generated, from plate to plate (see fig. 11).

These tracks are however, of extremely low brightness, and, though directly visible they do not have sufficient intensity to be detected with the commonly employed films (P30, TRIX).

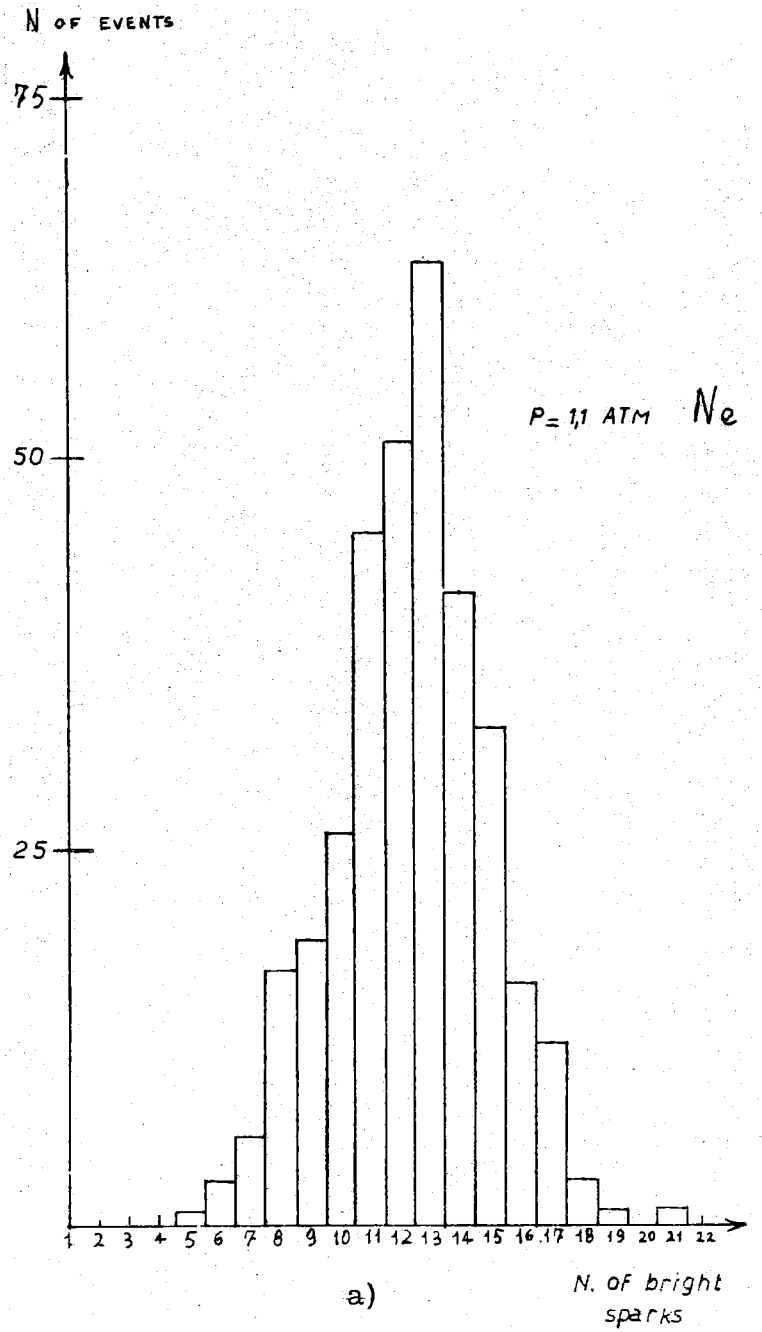
N OF EVENTS
75
50
25
P= 1,1 ATM Ne
1 2 3 4 5 6 7 8 9 10 11 12 13 14 15 16 17 18 19 20 21 22
N. of bright sparks

a)

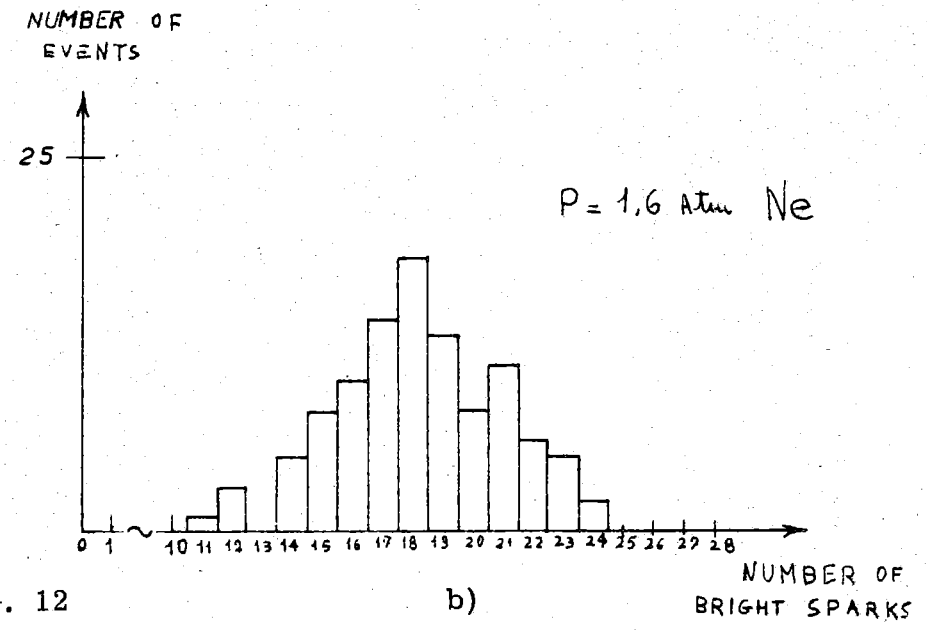
NUMBER OF EVENTS
25
P= 1,6 Atm Ne
0 1 10 11 12 13 14 15 16 17 18 19 20 21 22 23 24 25 26 27 28
NUMBER OF BRIGHT SPARKS

b)

FIG. 12

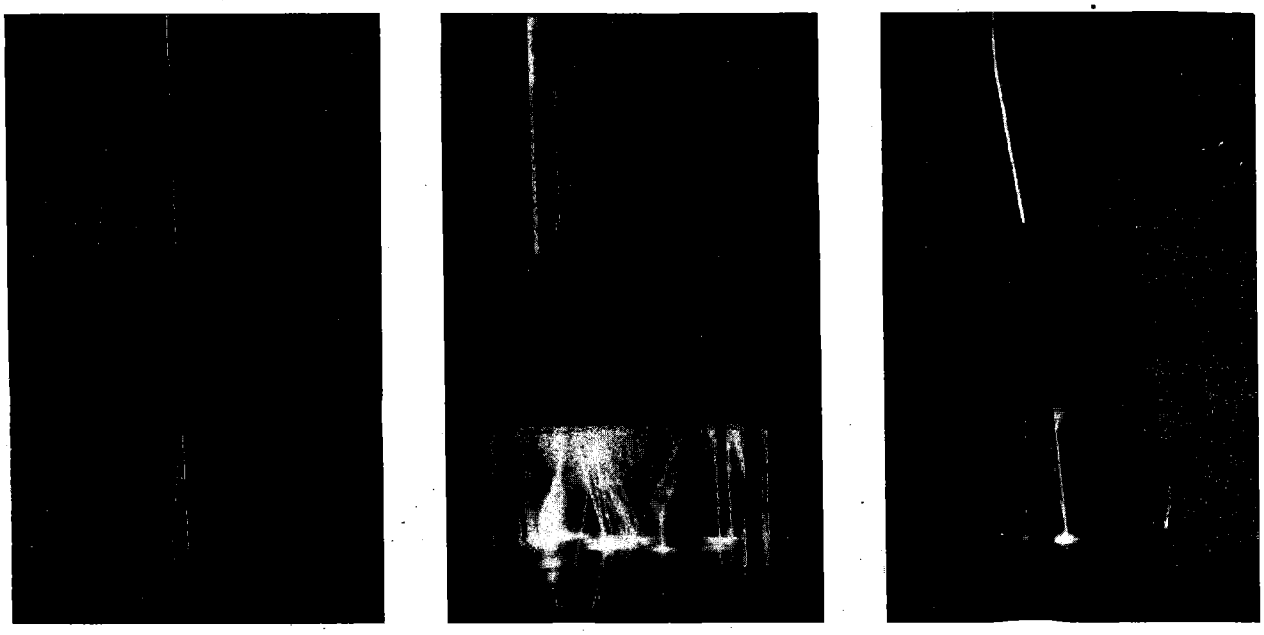

a) b) c)

Gas He
Upper chamber p = 600 mmHg
Lower chamber p = 1 atm
F/11 D = 1.5 m

FIG. 13

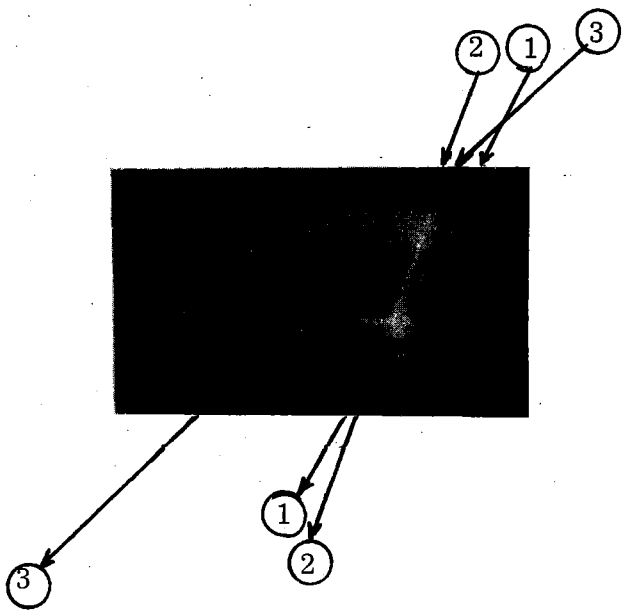

Gas He p = 1 atm
TRIX F/11 D = 1.5 m

FIG. 14

The picture of fig. 11 have been made using polaroid 3000 ASA films, f number of 1 : 1.1, distance d $\sim$ 0.5 m.

Realisation of a thin plates single gap spark chamber. -

We have constructed a prototype of a particularly simple wide gap spark chamber: one mylar sheet, 3 mils thick, has been cut and joined to form a parallelepiped of $20 \times 20 \times 10$ cm^3 size. This box, in which the gas flowed through a pipe and a hole in the side wall, was put between two copper plates (25×25 cm^2) kept at a distance of 10 cm, by four small lucite bars (fig. 15).

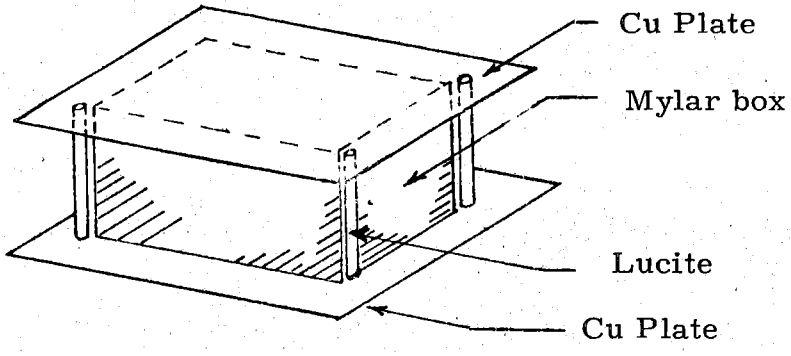

FIG. 15

Working with He in a 1 atm continuous flux, we observed an efficiency identical to that of the chamber previously described, there being no sensible difference in the sparks size.

We have made observations to detect two or more simultaneous tracks, both with the chamber described in a previous paragraph and with the latter thin wall chamber.

We have seen that in the latter there is a better efficiency in the case of two or more tracks.

In fact in the first chamber two tracks starting from the same point on the plate have a very different brightness, the brighter one being the one which is less inclined with respect to the electric field.

If the tracks do not start from the same point on the plate such an effect is less evident.

In the Mylar chamber the distribution of brightness between simultaneous tracks is more uniform.

Increasing the thickness of the insulator between the copper plates and the Mylar walls, with a 1 cm lucite slab, we further increased the efficiency for multiple tracks[4]. (see fig. 16).

Placing the lucite wall chamber above the thin wall chamber and interposing between them a lead shield, we observed in the upper one the primary ray track, and in the lower one the shower produced in the lead (see fig. 13).

With the Mylar chamber we have some examples of events similar to those of fig. 14.

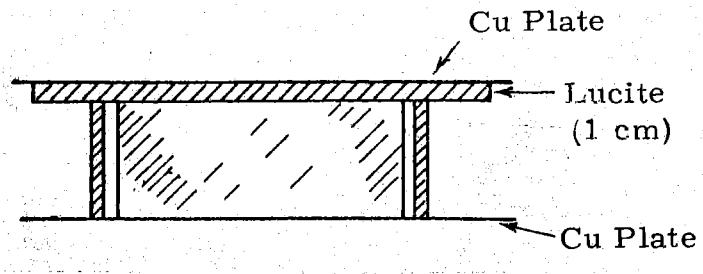

FIG. 16

In that picture we see three tracks: two making an angle $\varphi < 40^{o}$ with the electric field are detected in the ordinary way, the last one with $\varphi > 40^{o}$, is detected through the display of bright spots previously mentioned. This picture demonstrates a property of the chamber, that is contemporany particle tracks forming an arbitrary angle ($\theta < \varphi < 90^{o}$) with E can be detected.

References. -

(1) - Borisov, Dolgoshein and Luchkov, PTE 2, 170 (1962); Alikhanian et. al., Phys. Letters 4, 295 (1963).
(2) - Peter et al., Nuclear Instr. and Meth. 20, 201 (1963).
(3) - S. Fukuj and S. Haykawa, J. Phys. Soc. Japan 15, 532 (1960); J. U. Burnham et al., J. Sci. Instr. 40, 196 (1963).
(4) - S. Fukuj and S. Mijamoto, Nuovo Cimento 11, 113 (1959); S. Fukuj and B. Zacharov, Nuclear Instr. and Meth. 23, 24 (1963); A. I. Alikhanian et al., Phys. Letters 7, 272 (1963).
(5) - B. A. Dolgoshein et al., Strimernaia Kamera, Inst. of Phys. "Lebedev", Moscow (1964).
(6) - Bella et al., Nuovo Cimento 10, 1338 (1953).
(7) - T. E. Cranshaw and I. F. De Beer, Nuovo Cimento 5, 1107 (1957).
(8) - A. Roberts, Some recent advances in spark chamber techniques, 9th Scint. and Semicond. Symp., Washington (1964).
(9) - M. I. Daion and G. A. Leksin, Sov. Phys. -Uspekhi 6, 428 (1963).

We wish to thank Prof. I. F. Quercia for his constant interest and support. We also wish to thank all the members of our group, in particular Mr. M. Cinti and Mr. P. L. Belli, for their technological contribution.